The Fourteenth International Conference on
Computational Structures Technology
23–25 August, 2022 | Montpellier, France

Proceedings of the Fourteenth International Conference on
Computational Structures Technology
Edited by B.H.V. Topping and J. Kruis
Civil-Comp Conferences, Volume 3, Paper 14.4
Civil-Comp Press, Edinburgh, United Kingdom, 2022, doi: 10.4203/ccc.3.14.4

Effects of Connector Modelling on Explicit Shell Finite Element Models of Cold-formed Steel Shear Walls

G. Alshamsi[1], L. Xu[1], Y. Shi[2], Y. Zou[3] and X. Yao[3]

[1]Departement of Civil and Environmental Engineering, University of Waterloo, Canada
[2]School of Civil Engineering, Chongqing University, China
[3]Chang'an University, Shaanxi, China

Abstract

The study presented herein is concerned with assessing the influence of connector elements on the behaviour of finite element models of high capacity cold-formed steel (CFS) shear walls. Recently, CFS shear walls have been used as an economic and light-weight seismic force resisting system (SFRS) in North America, however their applications are limited to mid-rise buildings. To push the state-of-the art, a preliminary testing programme of an innovative, higher-capacity CFS shear wall is conducted. The testing programme consists of monotonic and cyclic tests as well as screw connection assembly tests in double shear. Furthermore, explicit shell finite element models of the shear walls were developed and calibrated with the experimental results. Finally, a parametric study on the type of connector element was carried out to assess the behaviour of the wall. The results indicate that representing the screw-fastened connections using three uncoupled springs gave the best numerical estimate.

Keywords: cold-formed steel, ABAQUS/Explicit, cycling loading, finite element, analysis, hysteresis energy, thin-walled structures, kinematic hardening,

1 Introduction

Owing to its durability and high strength-to-weight ratio, cold-formed steel (CFS) shear walls have emerged as an efficient and cost-effective seismic-force resisting system (SFRS) in North America. A conventional steel sheathed CFS shear wall consists of boundary studs and tracks (typically lipped channel sections), a steel

sheathing connected on one side of the frame, and hold-downs [1]. The system dissipates energy through a combination of screw bearing deformations and yielding of the sheathing. Currently, design standards restrict the use of CFS shear walls to low-rise and mid-rise buildings. For instance, the National Building Code of Canada [2] and limit the height of CFS structures to 20 meters. Moreover, conventional shear wall's capacity is limited due to eccentricities and single shear screw fastened connections. To achieve higher force levels, a new system is proposed that eliminates eccentricities and takes advantage of 3-ply connections.

Earlier attempts at quantifying the performance of CFS walls dates to the work performed by Serrette et al. [3]. The design values obtained from this study were incorporated in earlier versions of the AISI standard. More recently, tests on innovative CFS shear wall specimens were conducted by Santos & Rogers [4] and Brie & Rogers [5]. To achieve higher capacities, thicker material was used, and two original assemblies were proposed: a double-sheathed wall and a center-sheathed wall. The main findings indicate that the walls reached drift limits and capacities that were higher than values provided by AISI S400; and a preliminary design method to determine the bearing strength of 3-ply connections was also recommended. Finally, to address the lack of screw connection studies in double shear, Wu [6] and Zhang & Schafer [7] carried out laboratory tests for 3-ply connections including various combinations of steel thicknesses.

The primary objective of this paper is to assess the influence of screw modelling on the performance of a novel concentric-sheathed CFS wall. A testing program that comprises of full-scale test on shear wall specimens and connection assemblies was conducted, and explicit shell finite element models were developed and validated with the experimental results. The model was then analyzed with three different connector elements to propose the optimum modeling strategy.

2 Methods

The shear wall configuration investigated herein is shown in figure 1. The specimens comprise of a steel sheet concentrically placed between built-up hat studs and built-up angle tracks. The testing program was completed in collaboration with Chongqing University in China [8], where two specimens were constructed and subjected to a displacement-controlled monotonic (pushover) load and cyclic load. The observed failure modes include elastic and inelastic shear buckling of the sheet, buckling and fracture of chord studs at the face of the hold-downs; and finally, bearing and shear failure of the screw connections. Furthermore, cyclic and pushover tests were carried out on connection assemblies to determine the hysteretic and monotonic properties of the self-tapping screws used in the shear walls. The testing matrix is shown in table 1.

To gain insight on the walls' behaviour, shell finite element models were developed using the finite element software package ABAQUS [8]. In this study, the explicit solver was employed since severe convergence issues were encountered with the implicit solver. Given that the explicit solver makes use of a diagonal mass matrix, there is no need to assemble and invert the global stiffness matrix in every iteration. Also, with special consideration, the explicit scheme can be used to solve quasi-static problems. The details of the FE model are discussed next.

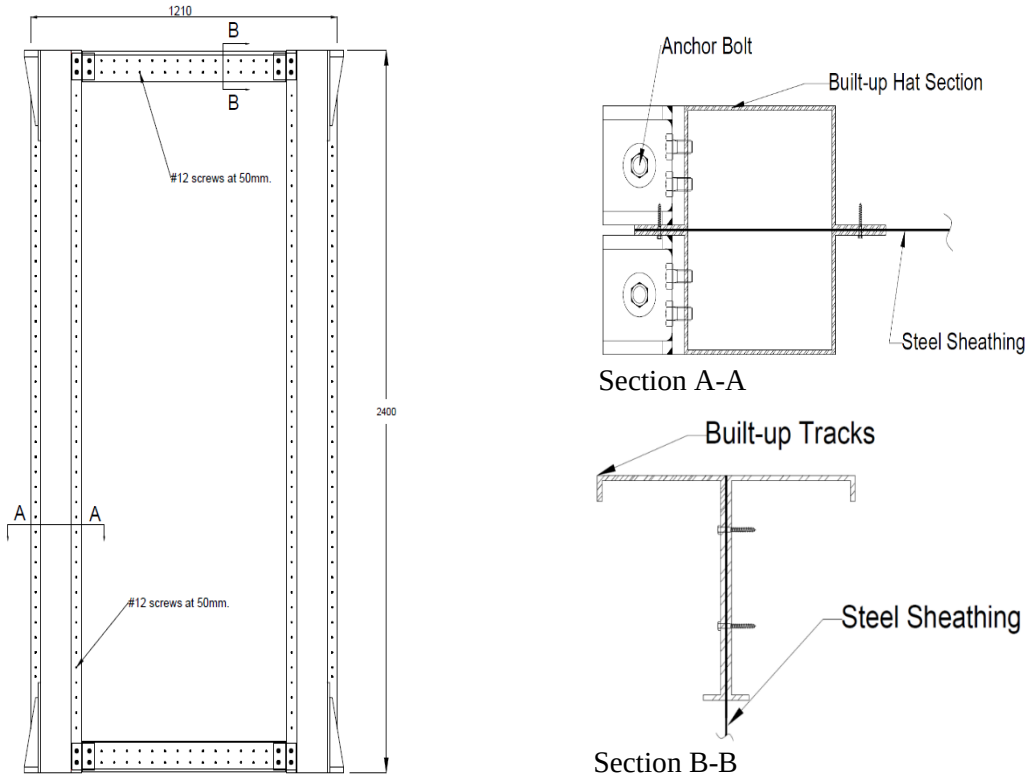

Figure 1: Structural details of the shear wall specimens.

Configuration	Sheathing Thickness (mm)	Wall Length (mm)	Wall Height (mm)	Framing Thickness (mm)	Screw Spacing (mm)	Loading Type
GD-6	0.8	1210	2400	2.5	50	Monotonic
GD-19	0.8	1210	2400	2.5	50	Cyclic

Table 1: Test Matrix

All parts of the shear wall assembly were discretized using the S4R element. The S4R is a 4-noded, general-purpose conventional shell element with 6 degrees of freedom and linear shape functions. One of the limitations of the explicit solver is that it contains a simple material library. To model the cyclic pinching and stiffness degradation effects (i.e.: Bauschinger effect), a linear kinematic hardening model was employed. Since the linear kinematic hardening model is not available in the ABAQUS/Explicit library, the constitutive model was defined using a user subroutine (VUMAT) which was retrieved from [9]. To simulate the experiment's conditions, nodes were defined in the bottom track and hold-downs at the exact location of the anchor bolts; and these nodes were restrained from moving in the X, Y and Z directions. On the other hand, the anchor bolts at the top track were bound to a

reference point using a kinematic coupling constraint. Finally, a displacement boundary condition was applied to the reference point.

The screw connections were modelled using three different elements: SpringA element, Cartesian connector element, and finally, beam multiple-point constraint (MPC_Beam). SpringA is a 2-noded axial-spring element that considers geometric non-linearities; hence the line of action can be rotated during the analysis rather than being fixed to one axis. Alternatively, the cartesian connector element represents each connection by three uncoupled nonlinear springs, two shear springs and a withdrawal spring. Lastly, MPC_beam models each connection as a rigid beam. The screws' material properties were defined as nonlinear force-displacement pairs which were obtained from the screw assembly test [10].

To ensure a quasi-static solution, the period of the first mode of the system was first obtained through a frequency extraction analysis. Then, the loading duration of the simulation was set to fifty times the period of the slowest mode. As shown in figure 2, the quasi-static response is verified by satisfying the energy balance criteria, which states that the ratio of kinetic and artificial energies to the internal energy of the system is limited to less than 5%.

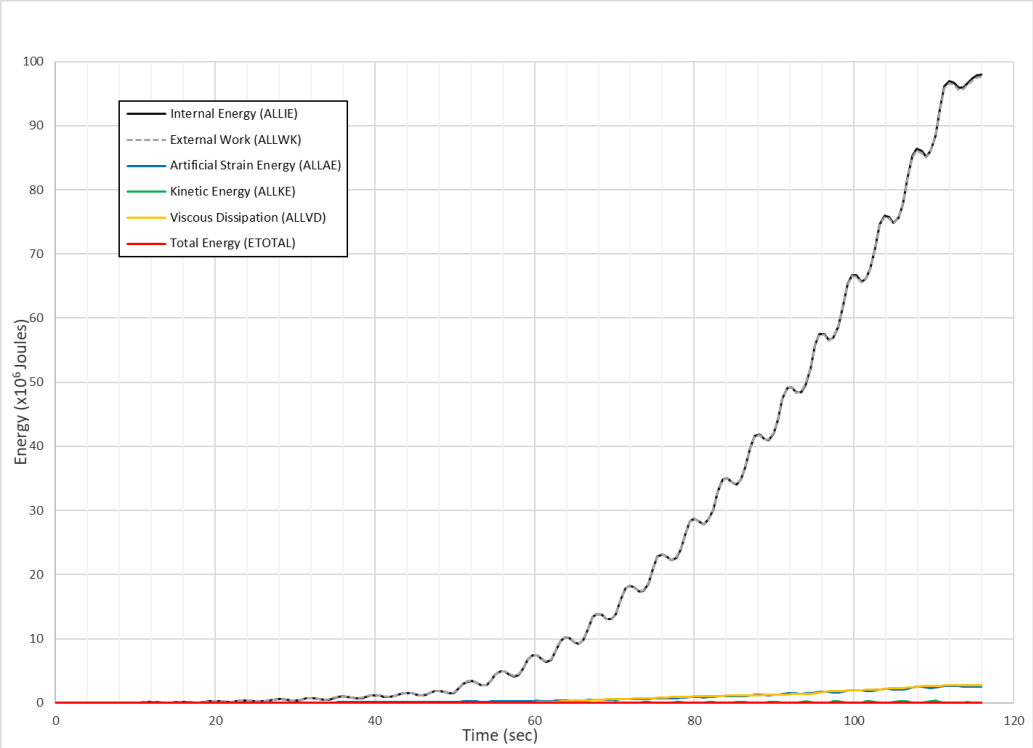

Figure 2: Energy output for the cyclic analysis.

3 Results

The results of the monotonic simulations are shown in figure 3, the model with springA connections greatly underestimates the stiffness and capacity of the shear wall. On the other hand, the graph of the model with MPC_Beam is characterized by a steep curve and a high peak load, which indicates that this type of connection

overpredicts the stiffness of the system. It's evident then that the cartesian element (three uncoupled springs) is the most appropriate modeling choice for this problem as the model predicted the peak load with very good accuracy (4% error), also while the model slightly overestimates the initial stiffness of the system, the overall response of the numerical simulation is comparable to the experimental results.

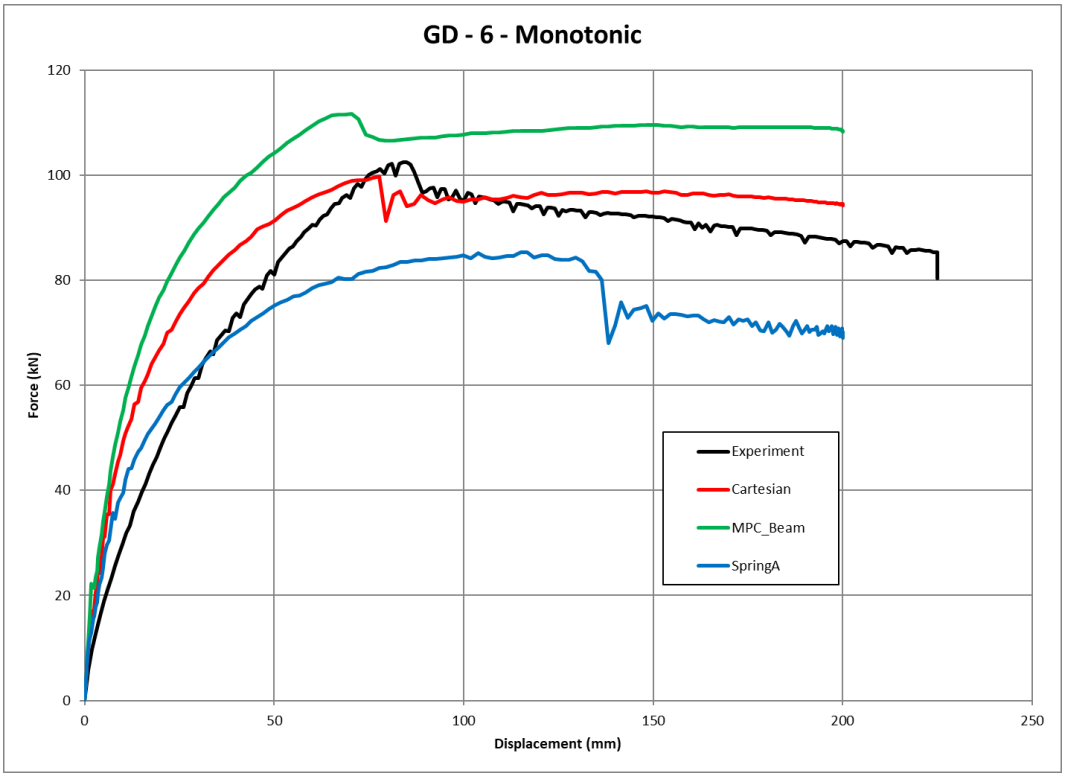

Figure 3: FEM vs experimental results for the monotonic test.

The same observations can be made for the cyclic simulations, as displayed in figures 4-6, the cyclic model with springA element is described by low peak load and a relatively "flat" unloading stiffness curve. Regarding the MPC_Beam model, the hysteresis loops have a more "rounded shape" than the loops obtained from the experiment which indicate that the numerical model is stiffer and able to dissipate more energy. The cartesian connector model overall shows the best agreement with the experimental results. Figure 7 shows isolated comparisons of cycles for the cartesian model, and it can be concluded that the model replicates the Bauschinger effect with reasonable accuracy. The main sources of error in the cyclic modelling can be credited to the energy dissipation mechanism. As previously stated, a CFS shear wall dissipates energy through yielding of the sheathing and screw bearing deformations. Therefore, from a numerical point of view, the sources of stiffness and strength degradation in the model are attributed to the constitutive material model and the choice of connector element. The linear kinematic hardening model is somewhat successful in modelling the hysteresis loops; however, to model the full severity of the Bauschinger effect, a connector element that is capable of modelling pinching and strength degradation parameters is essential. The current connector elements in the

ABAQUS library either define a screw backbone curve using pairs of force-deformation (springA, cartesian) or establish connections by eliminating degrees of freedom (multi-point constraints).

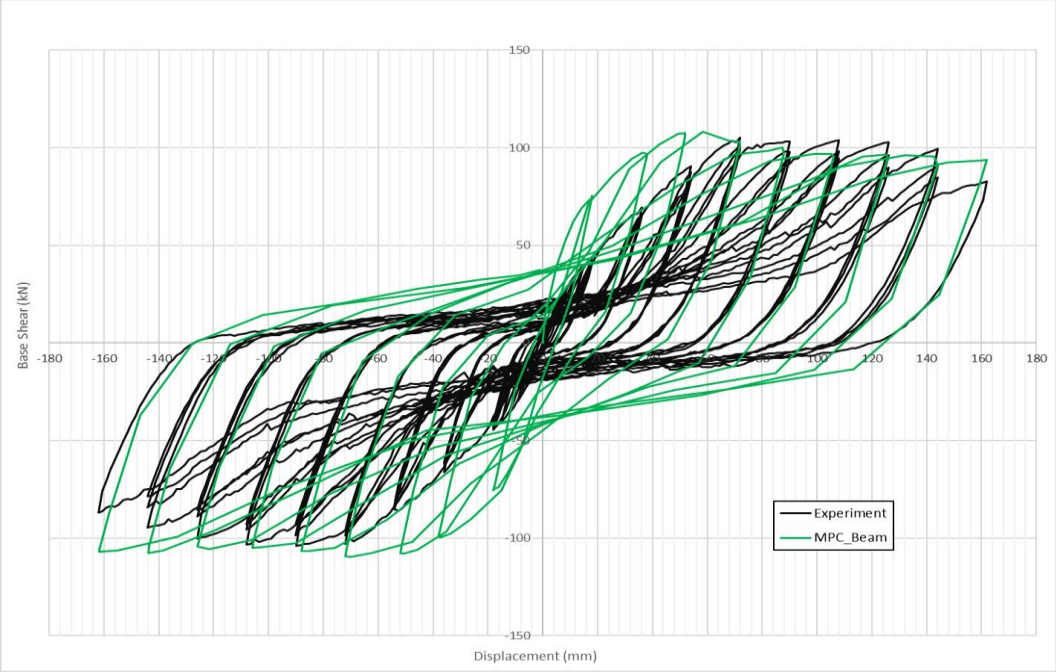

Figure 4: Cyclic experiment vs. FEM results (MPC_Beam).

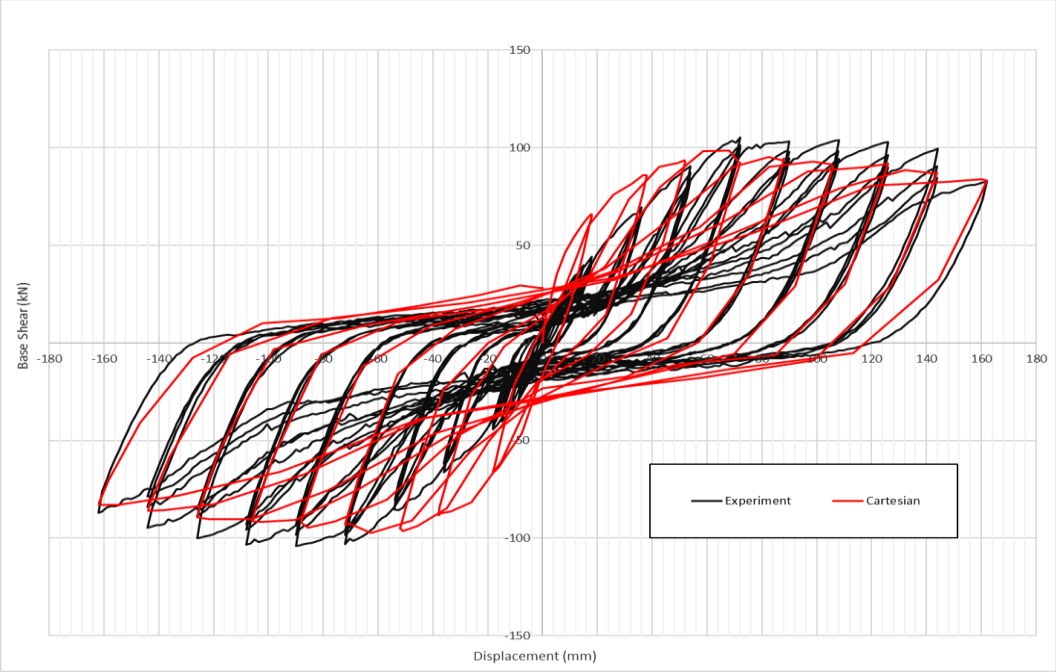

Figure 5: Cyclic experiment vs. FEM results (Cartesian).

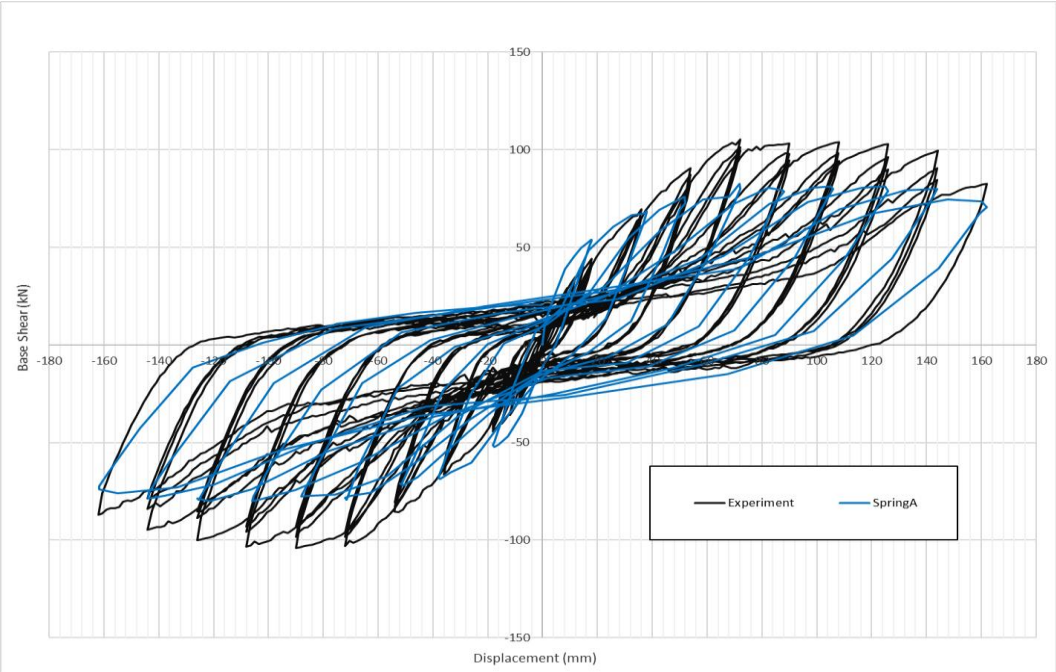

Figure 6: Cyclic experiment vs. FEM results (SpringA).

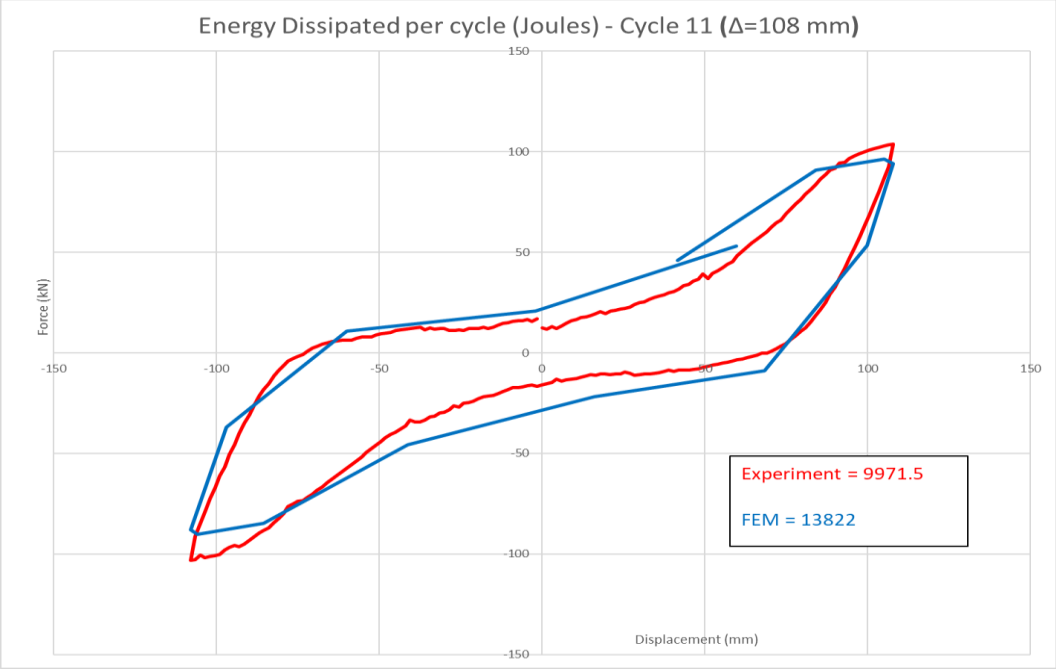

Figure 7: Energy comparison for hysteresis loops

4 Conclusions and Contributions

In this study, full-scale tests on an innovative high capacity CFS shear wall and 3-ply screw connection assemblies were carried out. In addition, a parametric study involving explicit shell finite element models were conducted to assess the influence

of screw connection modelling. The results indicate that representing screw connections with three uncoupled springs provides the best numerical estimate. The work herein emphasized the shortcomings of commercially available explicit finite element software packages, as currently there are no connector elements that can model the hysteretic pinching and strength degradation of CFS screw-fastened connections. Moreover, in the context of CFS shear walls as a main SFRS, this study also highlighted a pressing need to come up with a numerical method or an equation-based procedure to predict the strength of screw connections in double shear.

References

[1] AISI-D113-19, "Cold-Formed Steel Shear Wall Design Guide," Washington, DC, USA, 2019.

[2] NBCC, "National Building Code of Canada," Ottawa, ON, Canada, 2015.

[3] R. Serrette, J. Encalada, G. Hall, B. Matchen, N. Hoang and A. Williams, "Additional Shear Wall Values for Light Wegith Steel Framing," Santa Clara, CA, 1997.

[4] V. Santos and C. Rogers, "Higher Capacity Cold-Formed Steel Sheathed and Framed Shear Walls for Mid-rise Buildings: Part 1," Montreal, Quebec, Canada, 2017.

[5] V. Briere and C. Rogers, "Higher Capacity Cold-Formed Steel Sheathed and Framed Shear Walls for Mid-rise Buildings: Part 2," Montreal, Quebec, Canada, 2017.

[6] J. C. Wu, "Performance of Centre-sheathed Cold-formed Steel Framed Shear Walls Phase 2," McGill University, Quebec, 2019.

[7] Z. Zhang and B. W. Schafer, "Test Report: Cyclic Performance of Steel Sheet Connections for CFS Steel Sheet Shear Walls," The Cold-Formed Steel Research Consortuim, 2020.

[8] Hibbit, Karlsson and Sorenson, "ABAQUS/Explicit User's Manual," Hibbit, Karlsson & Sorenson Inc., Rhode Island, 2002.

[9] M. R. Behbahanifard, G. Y. Grondin and A. E. Elwi, "Experimental and Numerical Investigation of Steel Plate Shear Wall," Univeristy of Alberta, Edmonton, Calgary, 2003.

[10] Y. Xinmei, "Research on the Seismic Performance of Multi-storey Cold-formed Steel-Steel Plate Shear Wall Structure," PhD Thesis, Chang'an University, Xi'an, China, 2021.